

Characterization of plastic scintillator tiles equipped with SiPMs for the High Energy cosmic-Radiation Detection (HERD) experiment

A. De Benedittis^{c,d}, P. de la Torre Luque^{a,b,}, F. de Palma^g, M. Di Santo^{c,d}, L. Di Venere^{b,**}, P. Fusco^{a,b}, F. Gargano^{b,**}, F. Giordano^{a,b}, F. Loparco^{a,b}, S. Loporchio^{a,b}, M. N. Mazziotta^b, M. Mongelli^b, D. Serini^{a,b}, G. Torralba Elife^{e,f}, Z. M. Wang^{e,f}**

^aDipartimento Interateneo di Fisica dell'Università e del Politecnico di Bari, Italy

^bIstituto Nazionale di Fisica Nucleare - Sezione di Bari, Italy

^cDipartimento di Matematica e Fisica "E. De Giorgi" dell'Università del Salento, Lecce, Italy

^dIstituto Nazionale di Fisica Nucleare - Sezione di Lecce, Italy

^eGran Sasso Science Institute

^fIstituto Nazionale di Fisica Nucleare - Laboratori Nazionali del Gran Sasso

^gIstituto Nazionale di Fisica Nucleare - Sezione di Torino, Italy

The High Energy Cosmic Radiation Detection (HERD) facility onboard the future China's Space Station (CSS) will provide high quality data on charged cosmic rays and gamma rays reaching the measured range from few GeV to PeV energies. Because of this capability, HERD experiment would give a valuable contribution in several scientific topics as dark matter searches, study of cosmic ray chemical composition and high energy gamma-ray observations. The entire instrument is supposed to be surrounded by a plastic scintillator detector (PSD) which will be used to discriminate charged from neutral particles in order to correctly identify gamma-rays and nuclei. One configuration proposed and studied for the HERD PSD detector is the geometry of scintillator segmented in tiles and coupled to Silicon Photomultipliers (SiPMs). SiPMs provide similar or even better performances to the standard photomultiplier tubes (PMTs) with lower power consumption and cost benefits. In 2018, beam test campaigns were performed at CERN PS and SPS to test two prototypes of plastic scintillator tiles, equipped with a set of SiPMs. One was tested with a beam of electrons and pions and another prototype with an ion beam.

In the first prototype we studied the dependence of the collected light on the impact point of the beam particles and in the second one we tested the capability of the PSD to discriminate the ion charges. These results are presented.

*36th International Cosmic Ray Conference -ICRC2019-
July 24th - August 1st, 2019
Madison, WI, U.S.A.*

** Corresponding authors: pedro.delatorreluque@ba.infn.it, Fabio.Gargano@ba.infn.it,
Leonardo.Divenere@ba.infn.it

1. Introduction

Nowadays gamma-ray and cosmic-ray satellite experiments make use of plastic scintillators in order to discriminate charged and neutral particles and to identify nuclei. Existing gamma-ray telescopes, such as Fermi-LAT and DAMPE, employ these systems as anti-coincidence and also for ion identification [1, 2]. Other experiments, such as AMS-02, exploit the plastic scintillators to distinguish the charge of the arriving particles measuring their energy loss in the scintillator.

Usually, these scintillators are read out using photomultiplier tubes (PMTs), requiring high operation voltages (order of kV) and making them unpractical to be operated on satellites. However, recent developments in the field of Silicon Photomultipliers (SiPMs) are demonstrating that they can be suitable for the detection of fast light signals, with lower power consumption and showing very good sensitivity to low light yields. Many tests are ongoing to study the coupling of scintillators to SiPMs, to be used for future missions such as e-Astrogam [3], AMEGO[4] and HERD [5]. In recent years some tests of scintillators coupled to SiPMs were already performed, exploring this possibility also for different applications[6, 7, 8], but more tests are necessary to optimize these systems to be competitive with the classical PMT readout.

HERD (High Energy Cosmic Radiation Detection facility) is one of the cosmic-ray experiments programmed to go onboard the China's Space Station. The main goals of HERD are the indirect detection of dark matter particles, study of composition of cosmic rays and high energy gamma-ray observations.

The telescope is composed by a 3-D cubic calorimeter (CALO) surrounded by microstrip silicon trackers (STKs) from five sides except the bottom. The CALO and STK are covered by the plastic scintillator detector (PSD). A Transition Radiation Detector (TRD) is also planned to be located on the lateral side.

The PSD is segmented in order to improve gamma-ray selection efficiency and it will be used as a veto for charged particles, measurement of cosmic ray Z and trigger for charged cosmic rays.

Currently two configurations are being studied for the PSD geometry, respectively based on scintillating bars and tiles.

In this work, we assembled and tested two different prototypes of plastic scintillator tile, coupled with SiPMs. For the first tile (see Figure 1), which we call "Tile 1", we studied the dependence of the collected light on the impact positions of charged particles using a beam of electrons and pions with variable energy at CERN PS and SPS facilities. For the second tile (hereafter called "Tile 2"), its response to a beam of nuclei is studied to test its capability to discriminate charges.

2. Scintillator tile preparation

As mentioned, two different tiles were tested. The Tile 1 has a squared shape with a side of 15 cm and a thickness of 1 cm. Two angles were cut at 2.5 cm from the corner as shown in the Figure 1. The Tile 2 has a squared shape with a side of 10 cm and thickness of 1 cm. The geometry of the tile is shown in Fig.1.

The scintillators were levigated and wrapped with a white paper as reflector and black paper as coverage. Small windows were cut in order to place SiPMs directly on the scintillator. For

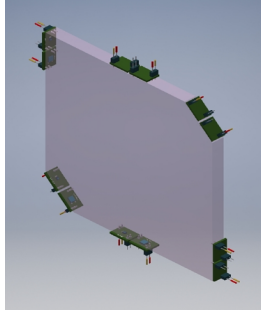


Figure 1: Tile 1 scheme and arrangement of SiPMs along it.

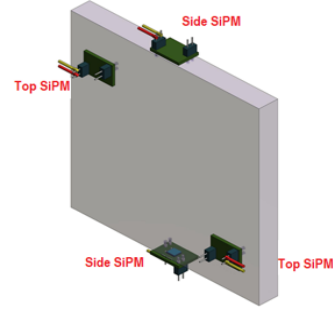


Figure 2: Tile 2 scheme and arrangement of SiPMs along it.

both tiles, BC-404 ([9]) plastic scintillator was used, which has a light yield of 68% of Anthracene and peak emission at 408 nm. The optical connection between the scintillator and the SiPM was achieved using BC-630 Silicone Optical Grease[10].

SiPMs produced by AdvanSiD sensitive to Near Ultraviolet (NUV) light with a $4 \times 4 \text{ mm}^2$ and a $1 \times 1 \text{ mm}^2$ area used in the Tile 1, placed along the edges, while only $4 \times 4 \text{ mm}^2$ SiPMs were used in the Tile 2 placed on the frontal part (hereafter "top" SiPMs) and on the edges ("side" SiPMs) (see Figure 2). They had a micro-cell pitch of $40 \mu\text{m}$. The photon detection efficiency (PDE) peaks at 420 nm, matching the BC-404 emission, with a maximum value of 43% which is reached at 5 V of over-voltage [11].

The Tile 1 was equipped with 12 SiPMs, 6 for each size, placed in different position of the tile perimeter, as shown in Figure 1. We will refer to the $4 \times 4 \text{ mm}^2$ SiPMs as "Large" SiPMs and $1 \times 1 \text{ mm}^2$ SiPMs as "Small" SiPMs.

Each SiPM was read-out using a trans-impedance amplifier produced by AdvanSiD[12] with an additional RC filter, optimized to cancel out the long recovery tail that characterizes these devices. Two amplification channels were available on the amplification boards (for both tiles), one with a gain 5 times larger than the other. We will refer to these channels as "High Gain" (HG) and "Low Gain" (LG). Then, The analog signals (twelve for the Tile 1 and eight for the Tile 2) were integrated and acquired with two Caen V792 QDCs [13].

2.1 Beam test setup

The tile 1 was tested at the CERN PS T10 beam line with 5 GeV/c particles and at the CERN SPS H8 beam line with 20 GeV/c particles. In both cases the beams were composed mainly by pions and electrons. A trigger system consisting of two plastic scintillators disposed along the beam line was implemented. At PS-T10, a plastic scintillator with a hole was used as halo veto in order to select a circular beam spot of 3 cm diameter. In this case, the tile was moved with respect to the beam line within 2 cm steps in order to irradiate the scintillator in different positions covering a grid of positions over all the tile and to study the dependence of the light collected by the SiPMs on the beam position. At SPS-H8 the tile was irradiated in the central position only.

The Second tile was tested at the CERN SPS H4 beam line with a beam of selected momentum of 330 GeV/Z, coming from a primary beam of lead, with energy 150 GeV/A, impinging onto a Beryllium target. A similar trigger system was used for this tile, adding another scintillator instead

of the one with the hole. This beam turned out to be mainly composed by particles with $Z=1$ and $Z=2$ (deuterium and helium respectively), but rich and with an almost flat composition in heavier nuclei with Z up to lead.

3. Data analysis and results

3.1 Calibration procedure

The calibration was performed using the dark count distributions measured in runs without particles. They arise because of the dark SiPM signals due to thermal noise, which causes random creation of electron-hole pairs. The charge distributions are characterized by discrete peaks, corresponding to 0, 1, 2, .. photons, depending on how many dark signals occur in the integration window. We fitted these dark distributions with multigaussian functions, as shown in Figure 3, in order to obtain the pedestal position (mean value of the first peak) and gain, defined as the average distance of consecutive peaks. To calibrate the signal distribution the pedestal is subtracted from the raw data and divided by the gain, allowing the conversion of ADC charge to detected photons.

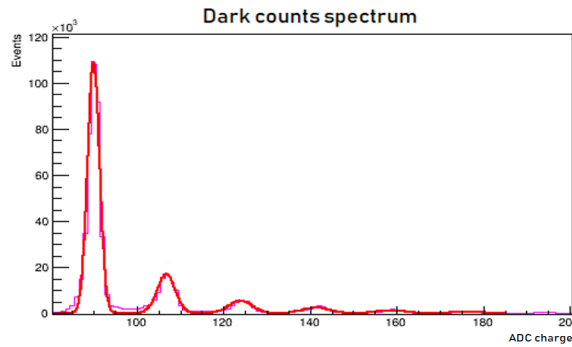


Figure 3: Example of pedestal distribution. The red line is the fitted multigaussian function.

3.2 Dependence of the response on the beam position

In this case, the Tile 1 was irradiated, at PS T10, in 33 different positions with beam spots of 3 cm diameter. In the case of small SiPMs the number of collected photons was very low (a few photons on average). The peak areas were fitted with a Poisson distribution, obtaining the average number of photons detected. In the case of large SiPMs the individual photon peaks could not be fitted individually, due to the higher intrinsic noise of the larger SiPMs and to the relative low statistics collected for each peak. A Landau distribution folded with a Gaussian function was used to fit the overall distribution. The ADC charge corresponding to the peak of the Landau function was then converted into photons with the conversion factors obtained in the calibration phase.

Plots in Figure 4 summarize the results obtained when changing the position in which we irradiated the tile for all large SiPMs. Each plot shows the number of photons detected by one SiPM in all the positions tested, which is indicated by the numbers inside the circles and by the color scale. The red boxes on the edges represent the position of the SiPM along the tile, with the numbers inside these boxes indicating the arbitrary index we assigned to each SiPM. The results

show that the detected number of photons is almost constant (30-40 photons) in all positions and for all SiPMs, with peaks in positions close to the SiPMs. Similar results were obtained for small SiPMs. However, in this case the number of detected photons (less than 3) was not sufficient to separate the particle signal from the pedestal.

3.2.1 Efficiency

As shown before, Large SiPMs provide a very good separation of pedestal and signal distributions and could be well suited to detect the passage of a charged particle. At SPS-H8 the tile was irradiated in the central position only to evaluate the detection efficiency. Individual photon peaks are visible up to more than 50 photons. From the ADC charge spectra, we evaluated the detection efficiency for minimum ionizing particles as a function of the threshold; very high efficiency (of the level of 99.999%) is easily reached with this simple configuration, fulfilling the requirements of anti-coincidence systems in cosmic ray satellites.

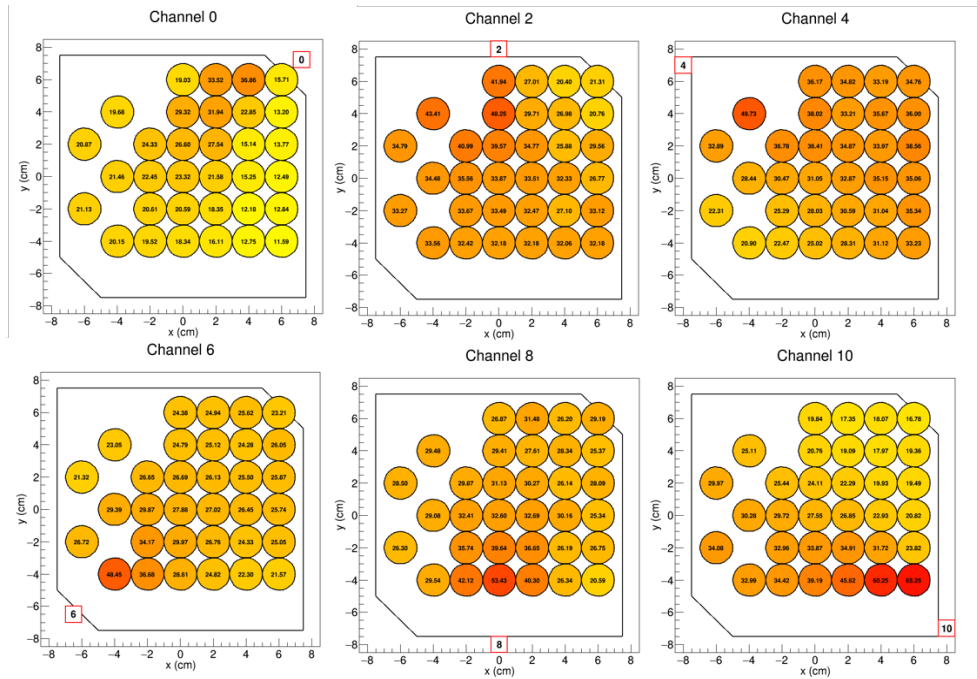


Figure 4: Maps summarizing the number of photons detected by each SiPM in the different beam positions tested. The numbers in the circles represent the detected photons, while the red boxes on the perimeter show the position of the SiPM.

3.3 Response to ion beam

The Tile 2 was placed along the ion beam line at SPS H4 in order to be irradiated in the central position. The signals were collected and calibrated for each SiPM for both amplification channels.

According to the Bethe Bloch formula, the energy released by charged particles in a dense material is proportional to the square of the charge Z of the particle. The spectra produced are expected exhibit by multiple peaks located according to a quadratic relation.

As mentioned above, we tested SiPMs in two different positions (side and top) with two amplification channels each. Figure 5 shows a comparison of the four configurations. Spectra were calibrated according to the procedure described in previous section.

First, it is evident that the side SiPMs show better resolution with respect to the top ones. In the case of the side SiPM, the high gain amplification appears to be inappropriate, since the readout chain saturates early and allows to resolve only up to $Z=3$, while the low gain case allows to resolve peaks up to $Z=6$.

On the other hand, the spectra for top SiPMs show an opposite behaviour, since high gain configuration seems more suitable to discriminate peaks. Simulations are currently undergoing to have a good understanding on this effect and its causes.

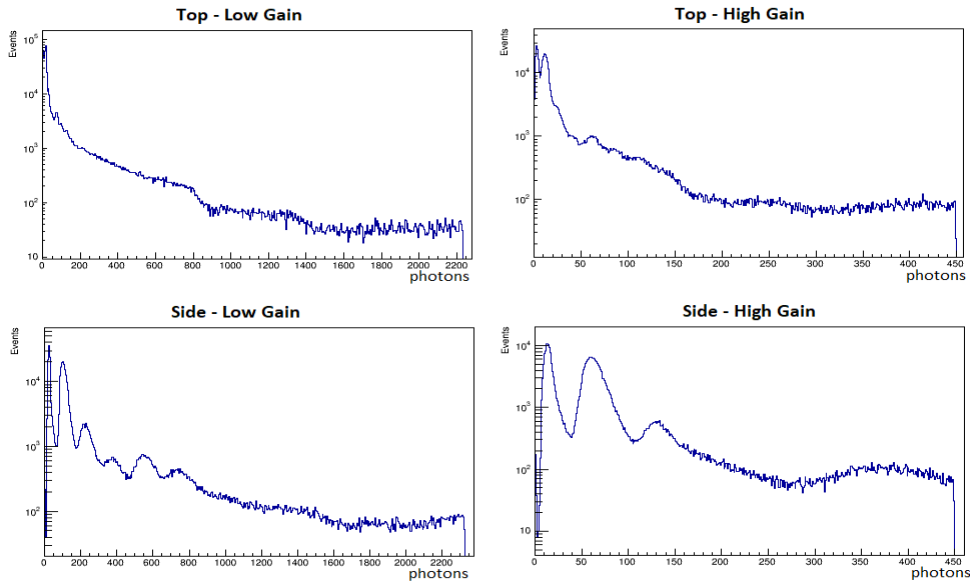


Figure 5: Comparison of the four different kinds of channel output. First row: Top SiPMs; second row: Side SiPMs; Left: Low gain channels; right: High gain channels.

In the spectrum of the Side-Low gain channel, it was usually possible to identify up to ten peaks before saturating the readout chain, even though only the first six peaks are well resolved, which means that nuclei up to carbon can be identified from this channel.

3.3.1 Channel associations

We combined the data coming from channels of the same type (e.g. Top - high gain, Top - low gain, etc.) by summing the calibrated signals event by event, to look for improvements in the resolution and number of resolved peaks.

Figure 6 shows the distributions obtained together with the plots showing the mean number of photons corresponding to each peak as a function of Z^2 . These plots show a linear fit (the expected behaviour of the deposited energy vs Z^2 from the Bethe-Bloch formula) and a fit using the Birks' law, which explains the saturation of a scintillator with deposited energy at high light yields. The formula used for the fit is $y = C + \frac{Nx}{(1+Kx)}$, where y stands for mean number of detected photons, x is Z^2 and K must be proportional to the Birks' constant.

We see a very clear improvement both in low and high gain for top SiPMs and a small improvement on the resolution of side SiPMs. In the distribution of the individual SiPMs we can hardly distinguish the first two peaks, while in the summed distribution we can fit more than 10 peaks. This behaviour is expected if we think to the combined channel as a SiPM with a larger area, which collects twice as much photons as the individual SiPMs.

We highlight that the calibration is crucial in order to have a good combination of independent channels. The good results obtained suggested that the calibration applied is correct.

On the other hand, the side SiPMs channels do not show any significant improvement. This might be due to the fact that one of the two side SiPMs shows much worse resolution than the other, which could arise from a not perfect optical contact of the SiPM with the scintillator.

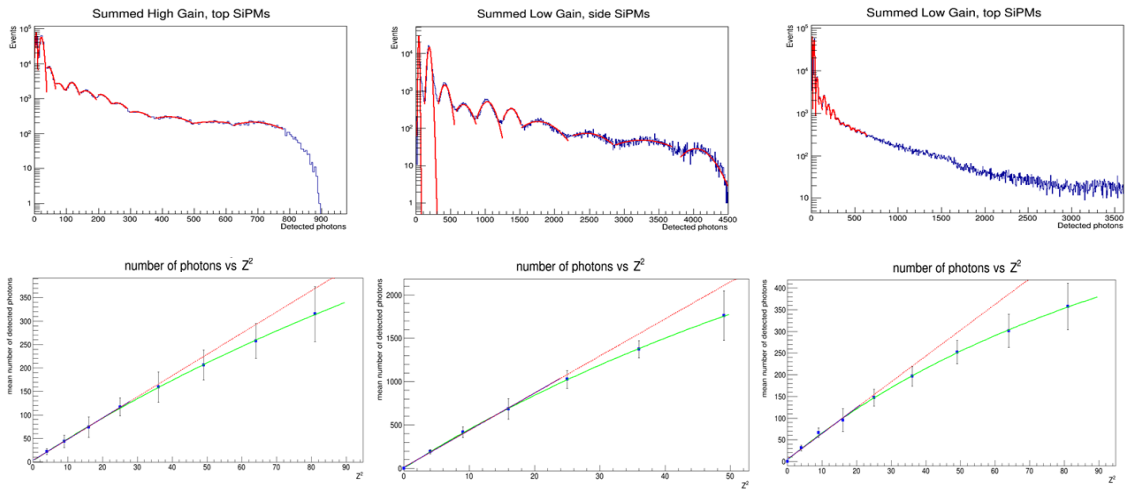


Figure 6: Fitted spectra of the associated channels Top - Low gain, Top - High gain and Side - Low gain. The lower plots show mean number of photons vs Z^2 . The green lines represent the best-fit curves obtained using Birks' formula; the blue lines are the linear fits in the range in which linearity is valid and the red dashed lines extend the linear fit for comparison with the green lines.

4. Conclusions

The measurements performed show that SiPMs can be coupled to scintillators to detect the passage of charged particles and to do charge identification. The $4 \times 4 \text{ mm}^2$ SiPMs proved to be appropriate to detect the passage of a minimum ionizing particle above the background since they show an efficiency always larger than 99.999%.

The beam position scan showed that the response is almost uniform in the tile, with the exception of the impact points close to the SiPM positions, for which the contribution of direct light is higher. This aspect must be taken into account when measuring the energy deposit in the scintillator. Finally, the detection efficiency achieved with this configuration is close to the requirements of ACD detectors for satellites (more than 99.999%). Improvements can be obtained by summing or implementing coincidence of multiple SiPMs.

The spectra in Figure 6 show that we can easily resolve up to an atomic number of ten using the single channels, having a better resolution for those SiPMs located at the edges of the tile compared

to those on the frontal part of the tile. For the latter, the density of photons reaching that face is too small, leading to a small statistics and smaller capability of charge discrimination.

In addition, summing up the equivalent channels, a clear improvement in the signal of the top SiPMs is observed, while the side SiPMs do not show significant changes. It was possible, using these associations, to identify $Z=9$, which is equivalent to fluorine. In conclusion, this study is showing that SiPM technology can be used instead of the classical PMTs to identify ions and that the resolution is improved if multiple SiPMs are combined.

More tests are planned in order to improve the tile assembly procedure, including different kind of wrapping and couplings to SiPMs, and to study different tile shape and SiPM configurations.

Acknowledgments

We would like to thank all the technical staff of the INFN Bari and in particular Mr. M. Franco and S. Martiradonna for their fundamental help in the mechanical realizations and during all the activities of the beam test.

References

- [1] Moiseev, A. A. et al. "The anti-coincidence detector for the GLAST large area telescope", *Astrop. Phys.* 27, 339 (2007).
- [2] Yu, Y. et al. "The plastic scintillator detector for DAMPE", *Astrop. Phys.* 94, 1 (2017).
- [3] De Angelis A., "The e-ASTROGAM mission. Exploring the extreme Universe with gamma rays in the MeV- GeV range", *Experimental Astronomy*, 44, 25 (2017).
- [4] AMEGO mission, <https://asd.gsfc.nasa.gov/amego/index.html>
- [5] Adriani, O. et al. "HERD proposal", <https://indico.ihep.ac.cn/event/8164/material/1/0.pdf>
- [6] Bohm, M. et al. "Fast SiPM Readout of the PANDA TOF Detector", *Journ. Instr.* 11, C05018 (2016).
- [7] Pooth, O. et al. "Scintillator tiles read out with silicon photomultipliers", *Journ. Instr.* 10, T10007 (2015).
- [8] Kaplin, V.A. et al. "Time and amplitude characteristics of large scintillation detectors with SiPM", *Phys. Procedia* 74, 232 (2015).
- [9] "BC-404 scintillator datasheet", <https://www.crystals.saint-gobain.com/sites/imdf.crystals.com/files/documents/bc400-404-408-412-416-data-sheet.pdf>
- [10] Saint-Gobain Crystals "Detector Assembly Materials", https://www.crystals.saint-gobain.com/sites/imdf.crystals.com/files/documents/detector-assembly-materials_69673.pdf
- [11] "AdvanSiD NUV SiPM datasheet", https://http://advansid.com/attachment/get/up_28_1432731773.pdf
- [12] AdvanSiD Transimpedance Amplifier, http://advansid.com/attachment/get/up_26_1386248853.pdf
- [13] "CAEN V792 QDC", <https://www.caen.it/products/v792/>